A pedagogical introduction to magnetic draping

Christoph Pfrommer[1]

in collaboration with

Jonathan Dursi[2]

[1] Heidelberg Institute for Theoretical Studies, Germany
Kavli Institute for Theoretical Physics, Santa Barbara
[2] Canadian Institute for Theoretical Astrophysics, Canada
SciNet Consortium, University of Toronto, Canada

Mar 24, 2010 / Galaxy Cluster Workshop, KITP

Outline

Outline

Why caring about magnetic fields?

Faraday rotation: B is dynamically irrelevant, $\beta \gtrsim 100$:

- B-topology determines strength of transport processes:
  heat, cosmic rays, ... $\rightarrow$ thermal structure, non-thermal radiative signatures, kinetic pressure contribution (buoyant instabilities)
- B-presence alters stability criterion for buoyancy:
  $\nabla_r S \rightarrow \nabla_r T$ (Balbus 2000, Quataert 2008, Parrish+2007+)
- B-amplification at fluid interfaces through "magnetic draping"
  (Lyutikov 2004, Dursi+2008, C.P.+2010)

$\rightarrow$ morphological features (filaments, stable bubbles, sharp interfaces) due to magnetic effects or ICM viscosity?

What is magnetic draping?

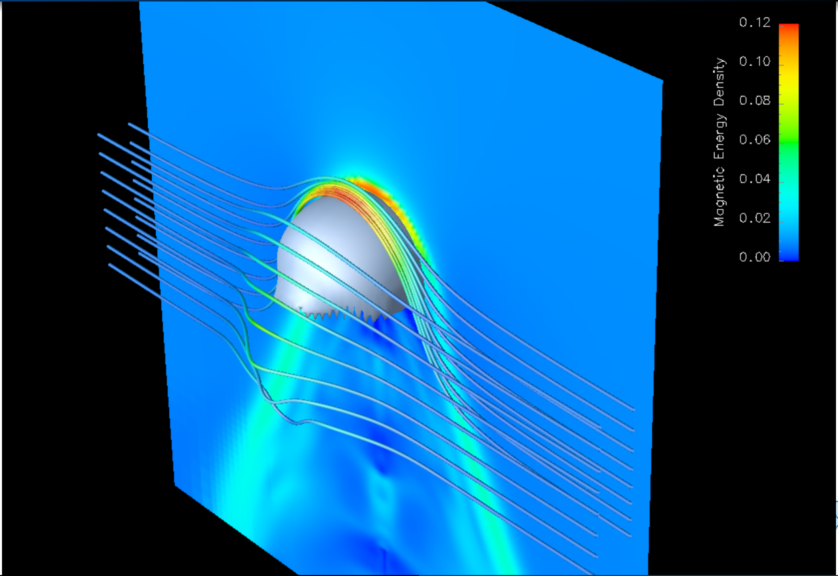

What is magnetic draping?

- Is magnetic draping (MD) similar to ram pressure compression?
  → no density enhancement for MD
  - analytical solution of MD for incompressible flow
  - ideal MHD simulations *(right)*
- Is magnetic flux still frozen into the plasma?
  yes, but plasma can also move along field lines while field lines get stuck at obstacle

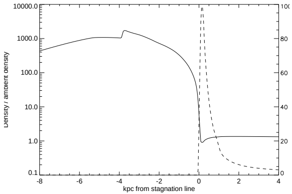

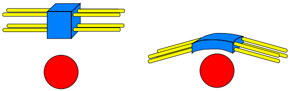

Applications of magnetic draping

- solar system: plasma physics
- hydrodynamic stability of radio bubbles
  (Dursi 2007, Ruszkowski+2007)
- sharpness (T_e, n_e) of cold fronts: without B, smoothed out by diffusion and heat conduction on $\gtrsim 10^8$ yrs
  (Lyutikov 2004, Dursi+2008)

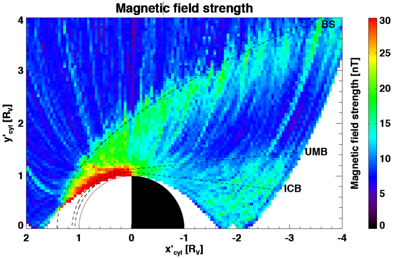

Guicking et al. (2010): magnetic draping around Venus

- magnetic draping on spiral galaxies: method for detecting the orientation of cluster fields (C.P.+2010)

Magnetic draping in 2D

Sometimes, 2D just isn't enough . . .

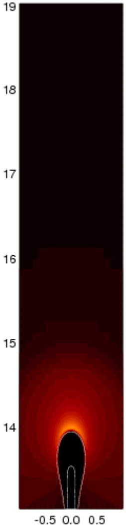

Potential flow around a moving sphere – 1

- origin $\mathcal{O}$ at the center of the sphere, constant inflow velocity $\boldsymbol{u}$
- incompressible ($\rho = \text{const}$): $\dot{\rho} + \text{div}\rho\boldsymbol{v} = 0 \quad \rightarrow \quad \text{div}\boldsymbol{v} = 0$
  $\boldsymbol{v} = \nabla\phi \quad \rightarrow \quad \Delta\phi = 0$
- boundary conditions: $\boldsymbol{v}\big|_\infty = \boldsymbol{0}$
- only solutions to $\Delta\phi = 0$ that vanish at infinity are $1/r$ and derivatives thereof with respect to the coordinates
- symmetry of the sphere $\rightarrow$ one constant vector in solution: $\boldsymbol{u}$
- linearity of $\Delta\phi = 0$ and boundary conditions $\rightarrow$ $\boldsymbol{u}$ can only enter linearly into ϕ: the only scalar that can be constructed is $\boldsymbol{u}\cdot\nabla\left(\frac{1}{r}\right)$
- ansatz: $\phi_\text{s} = \boldsymbol{A}\cdot\nabla\left(\frac{1}{r}\right) = -\frac{1}{r^2}\boldsymbol{A}\boldsymbol{e}_r$

Potential flow around a moving sphere – 2

- ansatz: $\phi_\mathrm{s} = \boldsymbol{A} \cdot \nabla \left(\frac{1}{r}\right) = -\frac{1}{r^2}\,\boldsymbol{A}\boldsymbol{e}_r$
- the surface of the body does not allow flow through it; determine $\boldsymbol{A}$ from boundary condition $(\boldsymbol{v} - \boldsymbol{u})\boldsymbol{e}_r\big|_{r=R} \overset{!}{=} 0$:
  $$\boldsymbol{v}\boldsymbol{e}_r\big|_{r=R} = \boldsymbol{e}_r^2 \partial_r \phi_\mathrm{s}\big|_{r=R} = \frac{2}{r^3}\boldsymbol{A}\boldsymbol{e}_r\big|_{r=R} \overset{!}{=} \boldsymbol{u}\boldsymbol{e}_r \quad \rightarrow \quad \boldsymbol{A} = \frac{1}{2}\,R^3\boldsymbol{u}$$
- potential in sphere-centered coordinate system: $\phi_\mathrm{s} = \frac{R^3}{2r^2}\,\boldsymbol{u}\boldsymbol{e}_r$
- transforming to lab system: $\phi_\mathrm{trans} = -uz = -ur\cos\theta = -r\boldsymbol{u}\boldsymbol{e}_r$
- potential $\phi = \phi_\mathrm{s} + \phi_\mathrm{trans} = -\left(\frac{R^3}{2r^2} + r\right)\,\boldsymbol{u}\boldsymbol{e}_r$
- $\boldsymbol{v} = \nabla\phi = \boldsymbol{e}_r\partial_r\phi + \boldsymbol{e}_\theta\frac{1}{r}\partial_\theta\phi =$
  $$\boldsymbol{e}_r\left(\frac{R^3}{r^3} - 1\right)\boldsymbol{u}\cdot\boldsymbol{e}_r - \boldsymbol{e}_\theta\left(\frac{R^3}{2r^3} + 1\right)\boldsymbol{u}\cdot\boldsymbol{e}_\theta = -\boldsymbol{u} + \frac{R^3}{2r^3}\,[3\boldsymbol{e}_r(\boldsymbol{u}\cdot\boldsymbol{e}_r) - \boldsymbol{u}],$$
  using $\boldsymbol{u} = \boldsymbol{e}_r(\boldsymbol{u}\cdot\boldsymbol{e}_r) + \boldsymbol{e}_\theta(\boldsymbol{u}\cdot\boldsymbol{e}_\theta) = \boldsymbol{e}_r u\cos\theta - \boldsymbol{e}_\theta u\sin\theta$ in the last step

Potential flow around a sphere vs. AMR simulation

v_x, v_y, v_z in the plane of the initial B-field

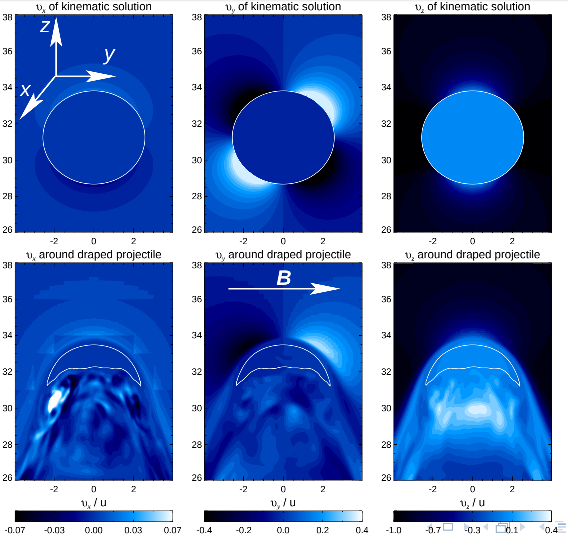

Exact MHD solution: kinetic approximation

$$\mathrm{curl}(\boldsymbol{v} \times \boldsymbol{B}) = \boldsymbol{0} \qquad \mathrm{div}\boldsymbol{B} = 0$$

- given our potential flow solution for the velocity field, we can solve for the magnetic field $\boldsymbol{B}$
- homogeneous magnetic field at $z = \infty$
- this yields four coupled, linear, homogeneous, first order partial differential equations which can be solved by the method of characteristics

Exact MHD solution: kinetic approximation

$$\mathrm{curl}(\boldsymbol{v} \times \boldsymbol{B}) = \boldsymbol{0} \qquad \mathrm{div}\boldsymbol{B} = 0$$

$$B_r = \frac{r^3 - R^3}{r^3} \cos\theta \left[C_1 \mp B_0 \sin\phi \int_\xi^r \frac{p(r,\theta) r'^4 \, \mathrm{d}r'}{(r'^3 - R^3 - p(r,\theta)^2 r')^{3/2} \sqrt{r'^3 - R^3}} \right],$$

$$B_\theta = \frac{2r^3 + R^3}{r^{5/2}\sqrt{r^3 - R^3}} \left[C_2 \pm 2B_0 \sin\phi \int_\xi^r \frac{r'^3 (r'^3 + 2R^3)\sqrt{r'^3 - R^3}\, \mathrm{d}r'}{(2r'^3 + R^3)^2 \sqrt{r'^3 - R^3 - p(r,\theta)^2 r'}} \right],$$

$$B_\phi = \frac{B_0 \cos\phi}{\sqrt{1 - R^3/r^3}}, \qquad p(r,\theta) = r \sin\theta \sqrt{1 - \frac{R^3}{r^3}},$$

where C_1 and C_2 are integration constants, ξ is the initial value for which B_r and B_θ are known, upper signs refer to the upper half-space and vice versa.

Approximate MHD solution near the sphere

$$\mathrm{curl}(\boldsymbol{v} \times \boldsymbol{B}) = \boldsymbol{0} \qquad \mathrm{div}\boldsymbol{B} = 0$$

$$
\begin{aligned}
B_r &= \frac{2}{3} B_0 \sqrt{\frac{3s}{R}} \frac{\sin\theta}{1+\cos\theta} \sin\phi, \\
B_\theta &= B_0 \sin\phi \sqrt{\frac{R}{3s}}, \\
B_\phi &= B_0 \cos\phi \sqrt{\frac{R}{3s}}, \qquad p(s,\theta) = \sqrt{3sR}\sin\theta
\end{aligned}
$$

where $s = r - R$. These equations uniformly describe the field near the sphere with respect to the angle θ.

MHD solution: kinematic approx. vs. AMR simulation

B_x, B_y, B_z in the plane of the initial B-field

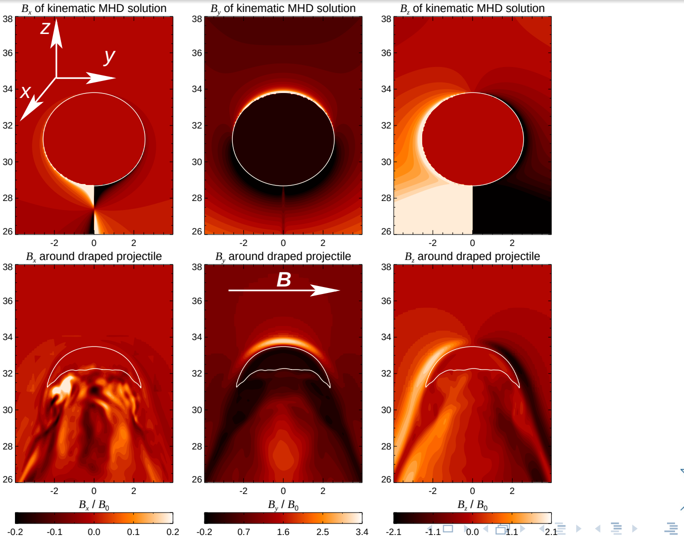

MHD solution: kinematic approx. vs. AMR simulation

B_x, B_y, B_z in the plane perpendicular to the initial B-field

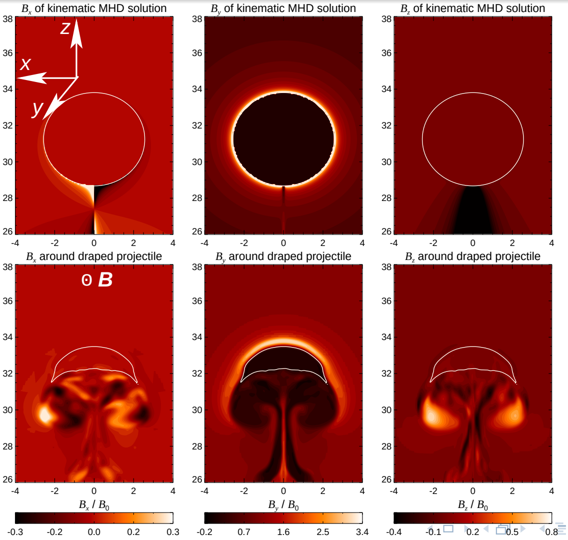

Thickness of the draping sheath - analytics

Energy density of magnetic draping sheath balances ram pressure:

$$
\begin{aligned}
B &= \frac{B_0}{\sqrt{1-\frac{R^3}{(R+s)^3}}} \approx \sqrt{\frac{R}{3s}}B_0 + \mathcal{O}\left(\sqrt{\frac{s}{R}}\right) \\
P_B &= \frac{B^2}{8\pi} = P_{B_0}\,\frac{R}{3s} = \alpha\rho_0 u^2 \\
\mathcal{M}_\mathrm{A}^2 &= \frac{u^2}{v_A^2} = \frac{\rho_0 u^2}{2P_{B_0}} = \frac{1}{2}\,\beta\gamma\mathcal{M}^2 \\
l_\mathrm{drape} &\equiv s = \frac{R}{6\alpha\mathcal{M}_\mathrm{A}^2} = \frac{R}{3\alpha\beta\gamma\mathcal{M}^2} \sim 100\,\mathrm{pc},
\end{aligned}
$$

for $R \simeq 30$ kpc, $\beta = P_\mathrm{th}/P_B \simeq 50$, and a trans-sonic flow, $\mathcal{M}^2 \simeq 1/\gamma$.

Thickness of the draping sheath – simulations

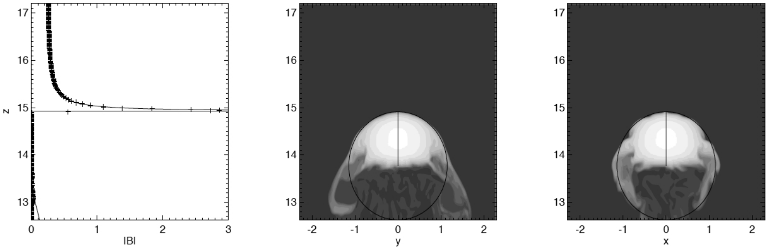

amplified draping field $B = \frac{1}{\sqrt{1-\frac{R^3}{r^3}}} B_0, \quad l_{\mathrm{drape}} \simeq \frac{R}{6\alpha\mathcal{M}_{\mathrm{A}}^2}$ with $\alpha \simeq 2$;

left: fitting peak position and a fall-off radius of the theory prediction; *right:* density cut-planes; circle shows radius and position given by the fit to the magnetic field structure, left;

$\rightarrow$ astonishing agreement of curvature radius at the working surface with potential flow predictions!

Magnetic energy of the draping layer

- in the draping layer, $\varepsilon_B \simeq \alpha\rho\upsilon^2$, is solely given by the ram pressure and *completely* independent of $\varepsilon_{\mathrm{icm}}$
- assume sphere with radius R and volume V_{sph}, constant thickness of the drape l_{drape} over an area $A = 2\pi R^2$:

$$
\begin{aligned}
E_{B,\,\mathrm{drape}} &= \frac{B_{\mathrm{drape}}^2}{8\pi} A\, l_{\mathrm{drape}} = \frac{B_{\mathrm{drape}}^2}{8\pi} \frac{A\,R}{6\alpha\,\mathcal{M}_A^2} \\
&= \alpha\rho\upsilon_{\mathrm{gal}}^2 \frac{A\,R}{6\alpha} \frac{B_{\mathrm{icm}}^2}{4\pi\,\rho\upsilon_{\mathrm{gal}}^2} = \frac{1}{2}\,\varepsilon_{B,\,\mathrm{icm}}\, V_{\mathrm{sph}}.
\end{aligned}
$$

→ "Archimedes principle of magnetic draping"

Streamlines in the rest frame of the galaxy

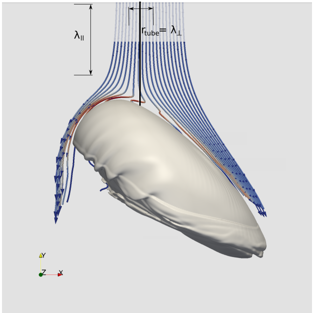

- Stokes function $p(s, \theta) = \sqrt{3sR}\,\sin\theta$ $\rightarrow$ critical impact parameter for $\theta = \pi/2$, $s = l_{\rm drape}$: $p_{\rm cr} = R/(2\mathcal{M}_A)$
- only those streamlines initially in a narrow tube of radius $p_{\rm cr} \simeq R/20 \simeq 1$ kpc from the stagnation line become part of the magnetic draping layer (color coded) $\rightarrow$ constraints on λ_B
- the streamlines that do not intersect the tube get deflected away from the galaxy, become never part of the drape and eventually get accelerated (Bernoulli effect)
- note the kink feature in some draping-layer field lines due to back reaction as the solution changes from the hydrodynamic potential flow solution to that in the draped layer

Conditions for magnetic draping

- ambient plasma sufficiently ionized such that flux freezing condition applies
- super-Alfvénic motion of a cloud through a weakly magnetized plasma: $\mathcal{M}_A^2 = \beta\gamma\mathcal{M}^2/2 > 1$
- magnetic coherence across the "cylinder of influence":

$$\frac{\lambda_B}{R} \gtrsim \frac{1}{\mathcal{M}_A} \sim 0.1 \times \left(\frac{\beta}{100}\right)^{-1/2} \quad \text{for sonic motions,}$$

Here R denotes the curvature radius of the working surface at the stagnation line.

Outline

1. Magnetic draping
    - Introduction
    - Physical insight
    - MHD Simulations

2. Spiral galaxies
    - Polarized radio ridges
    - Physics of magnetic draping
    - Draping and synchrotron emission

Polarized synchrotron emission in a field spiral: M51

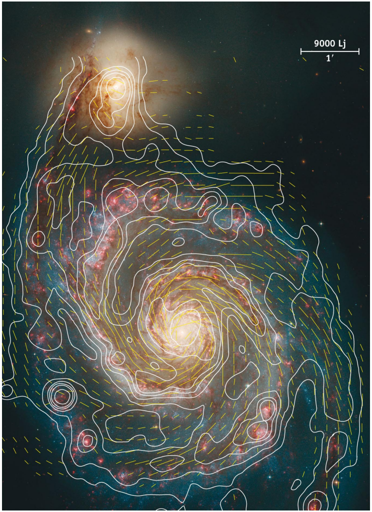

MPIfR Bonn and Hubble Heritage Team

- grand design 'whirlpool galaxy' (M51): optical star light superposed on radio contours
- polarized radio intensity follows the spiral pattern and is strongest in between the spiral arms
- the polarization 'B-vectors' are aligned with the spiral structure

Ram-pressure stripping of cluster spirals

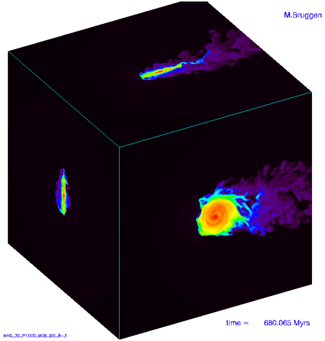

Brueggen (2008)

- 3D simulations show that the ram-pressure wind quickly strips the low-density gas in between spiral arms (Tonnesen & Bryan 2010)
- being flux-frozen into this dilute plasma, the large scale magnetic field will also be stripped

  → resulting radio emission should be unpolarized

Polarized synchrotron ridges in Virgo spirals

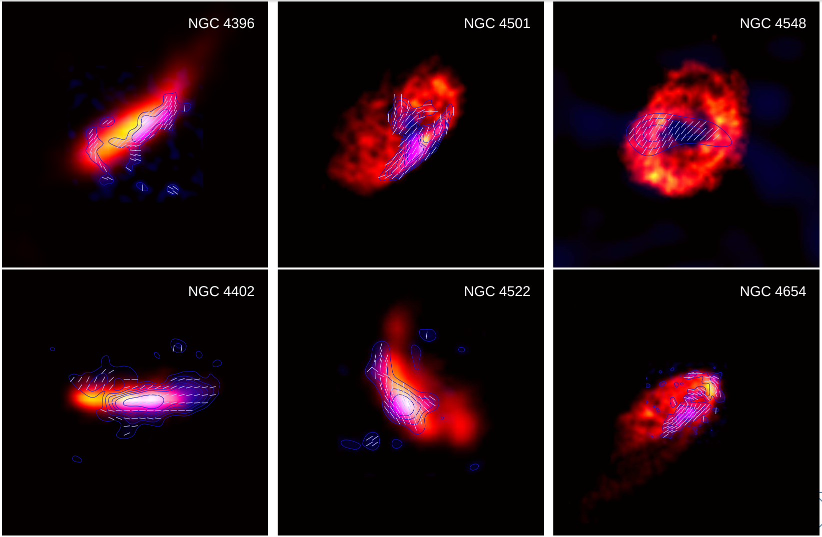

Vollmer et al. (2007): 6 cm PI (contours) + B-vectors; Chung et al. (2009): HI (red)

Magnetic draping around a spiral galaxy

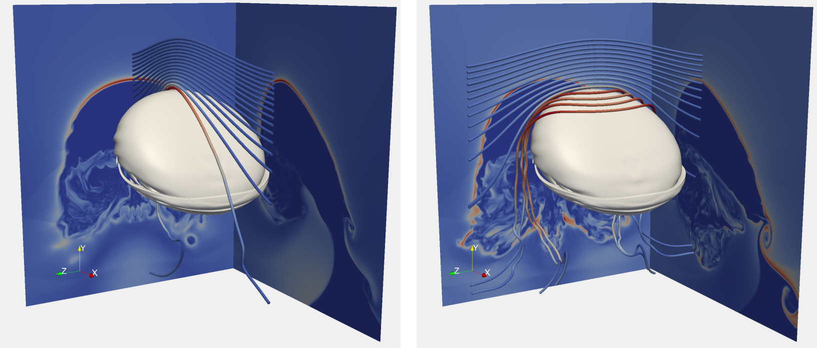

Athena simulations of spiral galaxies interacting with a uniform cluster magnetic field. There is a sheath of strong field draped around the leading edge (shown in red).

C.P. & Dursi, 2010, Nature Phys.

Magnetic draping around a spiral galaxy – physics

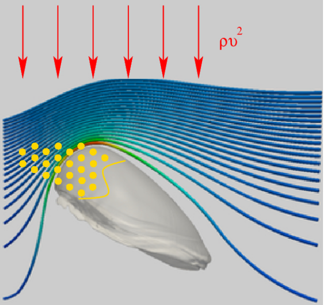

- the galactic ISM is pushed back by the ram pressure wind $\sim \rho \upsilon^2$
- the stars are largely unaffected and lead the gas
- the draping sheath is formed at the contact of galaxy/cluster wind
- as stars become SN, their remnants accelerate CRes that populate the field lines in the draping layer

- CRes are transported diffusively (along field lines) and advectively as field lines slip over the galaxy
- CRes emit radio synchrotron radiation in the draped region, tracing out the field lines there $\rightarrow$ coherent polarized emission at the galaxies' leading edges

Modeling the electron population

- cooling time scale of synchrotron emitting electrons (CRe):

$$\nu_{\rm sync} = \frac{3eB}{2\pi\, m_{\rm e} c}\,\gamma^2 \simeq 5\ \mathrm{GHz}\left(\frac{B}{7\,\mu\mathrm{G}}\right)\left(\frac{\gamma}{10^4}\right)^2,$$

$$\tau_{\rm sync} = \frac{E}{\dot{E}} = \frac{6\pi m_{\rm e} c}{\sigma_{\rm T} B^2 \gamma} = 5\times 10^7\ \mathrm{yr}\left(\frac{\gamma}{10^4}\right)^{-1}\left(\frac{B}{7\,\mu\mathrm{G}}\right)^{-2}$$

- typical SN rates imply a homogeneous CRe distribution (WMAP)
- FIR-radio correlation of Virgo spirals show comparable values to the solar circle: take MW CRe distribution inside our galaxies,

$$n_{\rm cre} = C_0\, e^{-(R-R_\odot)/h_R}\, e^{-|z|/h_z}$$

  with normalization $C_0 \simeq 10^{-4}\,\mathrm{cm}^{-3}$ as well as scale heights $h_R \simeq 8\,\mathrm{kpc}$ and $h_z \simeq 1\,\mathrm{kpc}$, normalized at Solar position
- truncate at contact of ISM-ICM, attach exp. CRe distribution $\perp$ to contact surface with $h_\perp \simeq 150$ pc (max. radius of Sedov phase)

Magnetic draping and polarized synchrotron emission

Synchrotron B-vectors reflect the upstream orientation of cluster magnetic fields

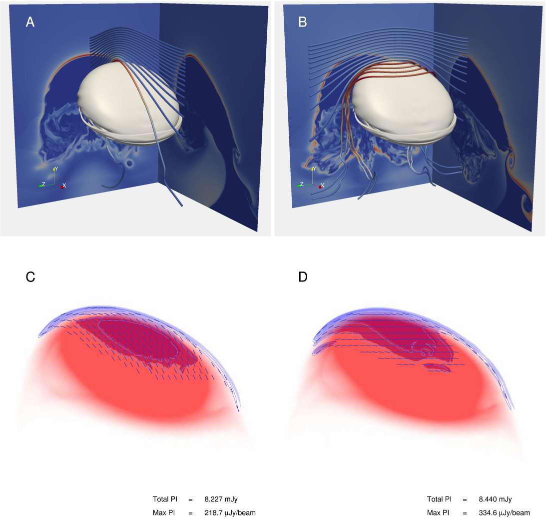

Simulated polarized synchrotron emission

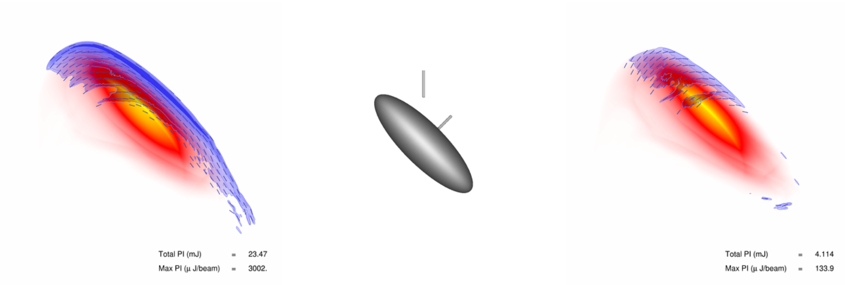

Movie of the simulated polarized synchrotron radiation viewed from various angles and with two field orientations.

Magnetic draping of a helical B-field

(Non-)observation of polarization twist constrains magnetic coherence length

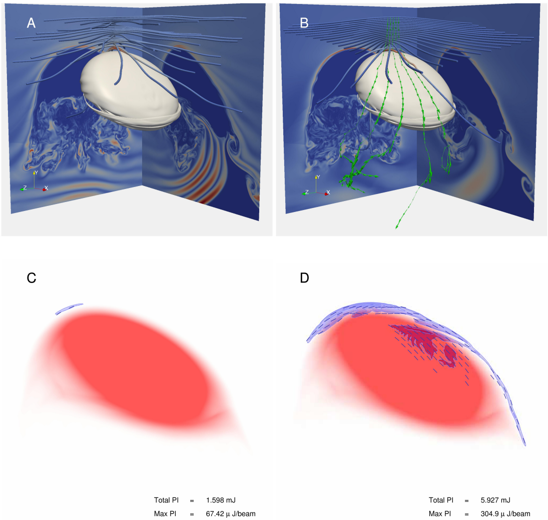

Magnetic coherence scale estimate by radio ridges

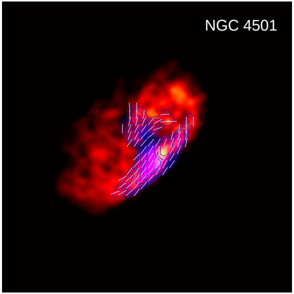

- observed polarised draping emission $\rightarrow$ field coherence length λ_B is at least galaxy-sized
- if $\lambda_B \sim 2R_{\text{gal}}$, then the change of orientation of field vectors imprint as a change of the polarisation vectors along the vertical direction of the ridge showing a 'polarisation-twist'
- the reduced speed of the boundary flow means that a small L_{drape} corresponds to a larger length scale of the unperturbed magnetic field ahead of the galaxy NGC 4501

$$L_{\text{coh}} \simeq \eta L_{\text{drape}} v_{\text{gal}} / v_{\text{drape}} = \eta \tau_{\text{syn}} v_{\text{gal}} > 100\,\text{kpc},$$

with $\tau_{\text{syn}} \simeq 5 \times 10^7$ yr, $v_{\text{gal}} \simeq 1000\,\text{km/s}$, and a geometric factor $\eta \simeq 2$

Varying galaxy inclination and magnetic tilt

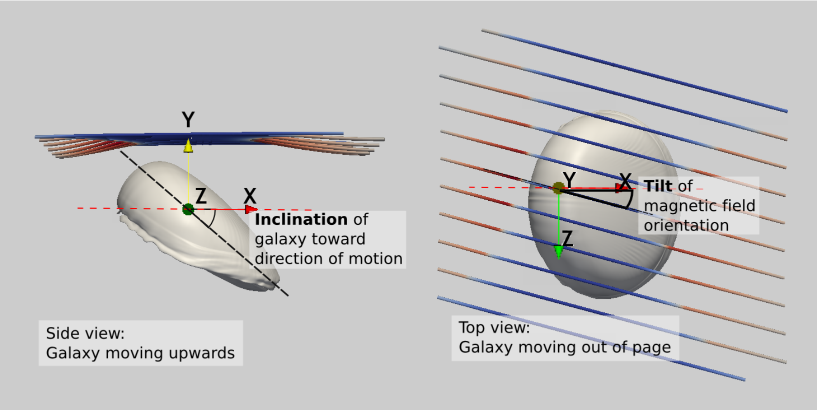

Observations versus simulations

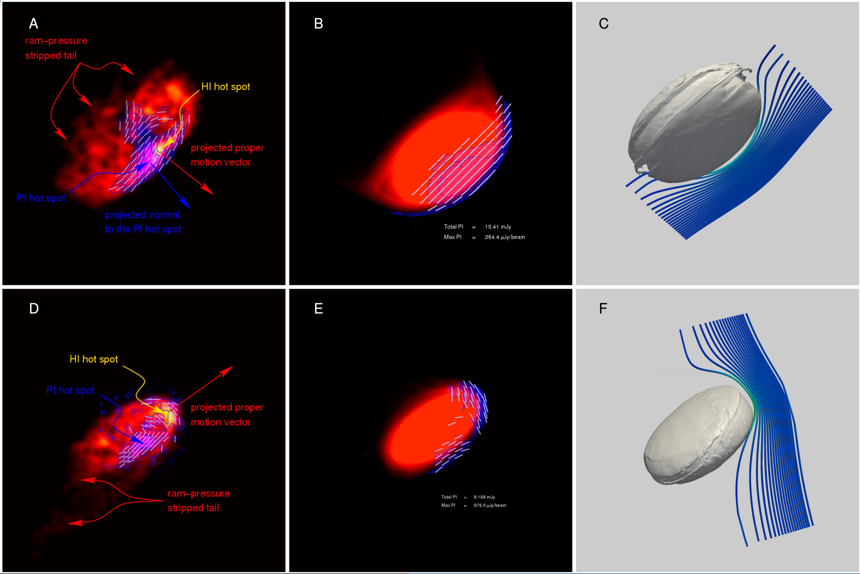

Biases in inferring the field orientation

- uncertainties in estimating the 3D velocity: v_r, ram-pressure stripped gas visible in HI morphology $\rightarrow \hat{\boldsymbol{v}}_\mathrm{t}$
- *direction-of-motion asymmetry:* magnetic field components in the direction of motion bias the location of $B_{\mathrm{max,\ drape}}$ (figure to the right): draping is absent if $\boldsymbol{B} \parallel \boldsymbol{v}_\mathrm{gal}$

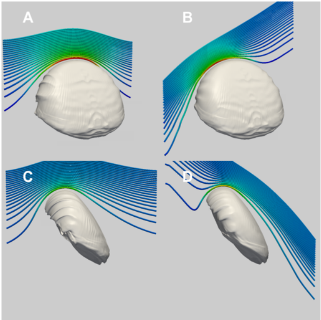

- *geometric bias:* polarized synchrotron emission only sensitive to traverse magnetic field B_t ($\perp$ to LOS) $\rightarrow$ maximum polarised intensity may bias the location of $B_{\mathrm{max,\ drape}}$ towards the location in the drape with large B_t

Mapping out the magnetic field in Virgo

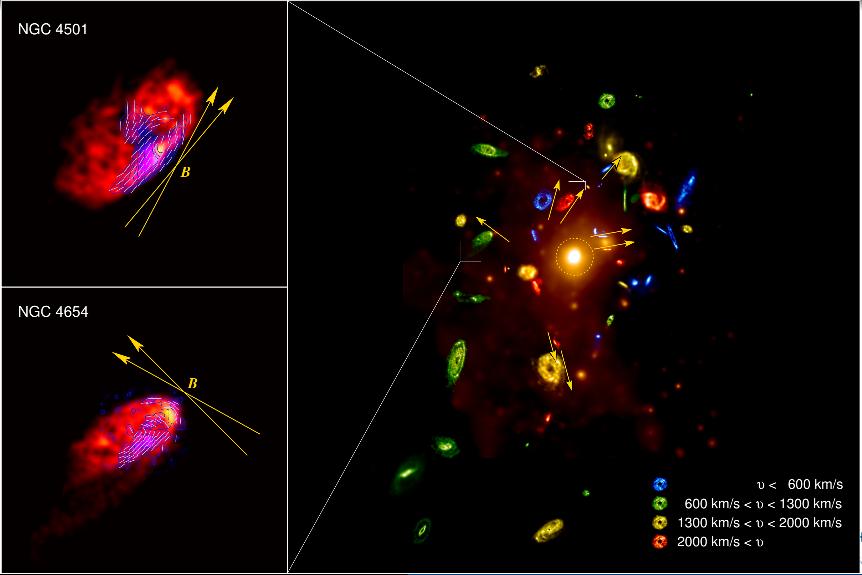

Discussion of radial field geometry

- The alignment of the field in the plane of the sky is significantly more radial than expected from random chance. Considering the sum of deviations from radial alignment gives a chance coincidence of less than 1.7% ($\sim 2.2\,\sigma$).
- For the three nearby galaxy pairs in the data set, all have very similar field orientations.

$\rightarrow$ Which effect causes this field geometry?

Magneto-thermal instability? (Parrish+2007, C.P.+2010)
Radial infall? (Ruszkowski+2010)

Gravitational shock wave heating

Observed temperature profile in clusters is decreasing outwards
$\rightarrow$ heat also flows outwards along the radial magnetic field.
How is the temperature profile maintained? $\rightarrow$ gravitational heating

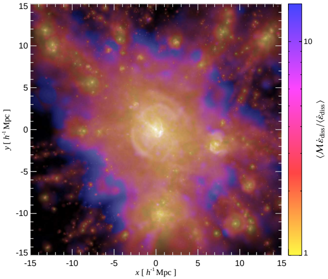

shock strengths weighted by dissipated energy

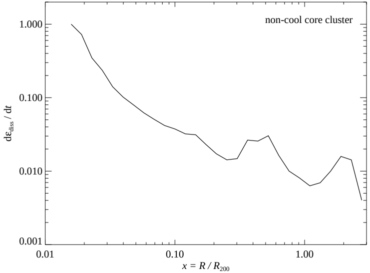

energy flux through shock surface $\dot{E}_{\rm diss}/R^2 \sim \rho \upsilon^3$
$\rightarrow$ increase towards the center

Conclusions on magnetic draping around galaxies

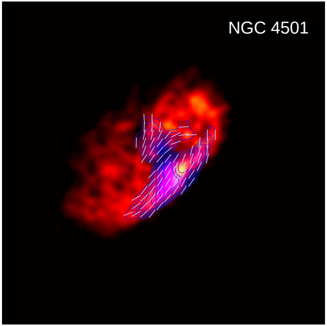

- draping of cluster magnetic fields naturally explains polarization ridges at Virgo spirals

Conclusions on magnetic draping around galaxies

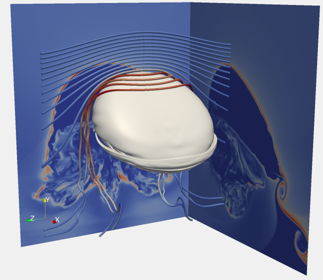

- draping of cluster magnetic fields naturally explains polarization ridges at Virgo spirals
- this represents a new tool for measuring the in situ 3D orientation and coherence scale of cluster magnetic fields

HITS

Conclusions on magnetic draping around galaxies

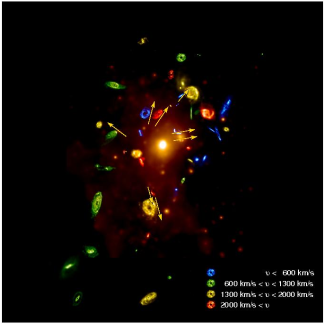

- draping of cluster magnetic fields naturally explains polarization ridges at Virgo spirals
- this represents a new tool for measuring the in situ 3D orientation and coherence scale of cluster magnetic fields
- application to the Virgo cluster shows that the magnetic field is preferentially aligned radially

Conclusions on magnetic draping around galaxies

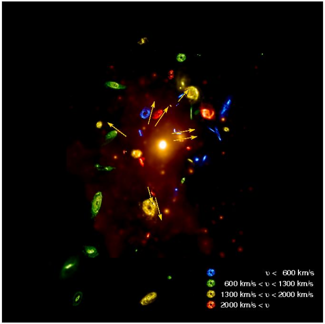

- draping of cluster magnetic fields naturally explains polarization ridges at Virgo spirals
- this represents a new tool for measuring the in situ 3D orientation and coherence scale of cluster magnetic fields
- application to the Virgo cluster shows that the magnetic field is preferentially aligned radially

- this finding implies efficient thermal conduction across clusters that stabilizes these non-cool core systems
- important implications for thermal cluster history → galaxy cluster cosmology

Literature for the talk

- Pfrommer & Dursi, 2010, Nature Phys., 6, 5206, *Detecting the orientation of magnetic fields in galaxy clusters*
- Dursi & Pfrommer, 2008, ApJ, 677, 993, *Draping of cluster magnetic fields over bullets and bubbles - morphology and dynamic effects*